Nanotechnology

PAPER

Dynamics of self-assembled cytosine nucleobases on graphene

IOP Publishing Nanotechnology

Nanotechnology **29** (2018) 195601 (9pp) https://doi.org/10.1088/1361-6528/aab0ea

Dynamics of self-assembled cytosine nucleobases on graphene

Nabanita Saikia[1], **Floyd Johnson, Kevin Waters** and **Ravindra Pandey**[1]

Department of Physics, Michigan Technological University, 1400 Townsend Drive, Houghton, MI 49931, United States of America

E-mail: nsaikia@mtu.edu and pandey@mtu.edu

Received 31 October 2017, revised 26 January 2018
Accepted for publication 20 February 2018
Published 13 March 2018

Abstract

Molecular self-assembly of cytosine (C_n) bases on graphene was investigated using molecular dynamics methods. For free-standing C_n bases, simulation conditions (gas versus aqueous) determine the nature of self-assembly; the bases prefer to aggregate in the gas phase and are stabilized by intermolecular H-bonds, while in the aqueous phase, the water molecules disrupt base–base interactions, which facilitate the formation of π-stacked domains. The substrate-induced effects, on the other hand, find the polarity and donor–acceptor sites of the bases to govern the assembly process. For example, in the gas phase, the assembly of C_n bases on graphene displays short-range ordered linear arrays stabilized by the intermolecular H-bonds. In the aqueous phase, however, there are two distinct configurations for the C_n bases assembly on graphene. For the first case corresponding to low surface coverage, the bases are dispersed on graphene and are isolated. The second configuration archetype is disordered linear arrays assembled with medium and high surface coverage. The simulation results establish the role of H-bonding, vdW π-stacking, and the influence of graphene surface towards the self-assembly. The ability to regulate the assembly into well-defined patterns can aid in the design of self-assembled nanostructures for the next-generation DNA based biosensors and nanoelectronic devices.

Supplementary material for this article is available online

Keywords: self-assembly, DNA nucleobases, graphene, molecular dynamics simulation

(Some figures may appear in colour only in the online journal)

1. Introduction

The self-assembly of biomolecules [1] and DNA/RNA nucleobases into well-defined hierarchical structures has been a topic of recent research interests [2, 3]. In particular, the structural organization of DNA nucleobases on 2D material surfaces has facilitated the wide scale applications of functionalized nanomaterials as biosensors [4, 5]. This is due to the recent advances in the fabrication techniques, which has facilitated the self-assembly of DNA nucleobases into well-defined hierarchical structures on metallic or nonmetallic surfaces [2, 6–10]. For example, the self-assembled heterostructures of DNA nucleobases on Au (111) [11, 12], Ag (111) [13], Cu(110 and 111) [14, 15], and highly ordered pyrolytic graphite (HOPG) [16, 17] have been recently fabricated. Such attempts on functional 2D materials including graphene are rather limited at both the experimental and theoretical levels. The literature finds the Scanning Tunneling Microscopy (STM) imaging of the self-assembly of guanine nucleobases on MoS_2 [18], while the self-assembly of DNA nucleobases on h-BN [19, 20], was studied using first principles density functional theory (DFT) methods. Due to the computational cost, DFT calculations have limitations in terms of the system size and explicit description of the solvent environments. It is to be noted that, atomistic simulations based on molecular dynamics (MD) method using classical

[1] Authors to whom any correspondence should be addressed.

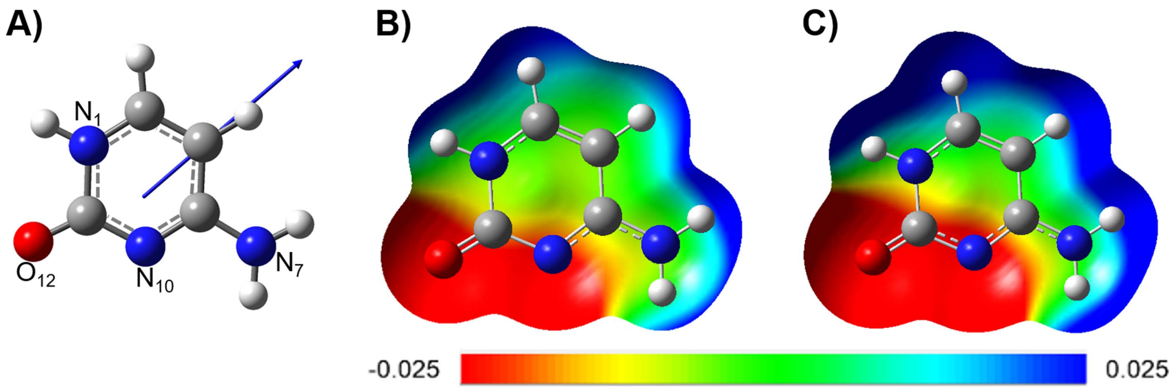

Figure 1. (A) Cytosine with its dipole moment vector orientation. The ESP isosurface of cytosine in (B) gas, and (C) aqueous phases.

force fields can be quite useful to understand the dynamics of a system, using modest computational resources as discussed in detail in [21].

In this study, we systematically investigate the self-assembly of cytosine (C_n) nucleobases on graphene using MD simulation methods with the objective to elucidate on the crossover mechanism for self-assembly, from free-standing to the surface supported cases that govern the base–base and base–surface interactions [22, 23]. Of the previously studied 2D nanomaterials, graphene is the material of choice, due to its inherent electronic properties that can be tailored via functionalization. It has been reported that a weakly interacting surface like graphene promotes the planar orientations of DNA bases on the surface [24, 25]. Thus, a fundamental understanding of the intermolecular interactions that determine the molecular assembly on graphene is required [26, 27].

Cytosine is a planar DNA nucleobase with a dipole moment and polarity that can facilitate interactions with the 2D surface of graphene to form stable heterostructures [28]. Cytosine depicts regions of negative electron density on the O_{12}, N_{10} atoms while N_1 and N_7 atoms are regions with intermediate to positive electron densities as shown in figures 1(B) and (C). Unlike guanine, which exhibits three H-bond acceptors and two H-bond donor sites in alternate positions [29], the donor and acceptor sites in cytosine is localized, lying adjacent to each other [30]. This configuration restricts the ability to form long-range ordered 2D monolayers through hydrogen bonding, while 1D structural motifs are conceivable [31].

The calculated results reveal the importance of H-bonding, π-stacking, role of graphene surface and the influence of simulation media towards the self-assembly of C_n bases. Moreover, the van der Waals π-stacking is predicted to play a key role in stabilizing the physisorption of cytosine on graphene. The intermolecular H-bonding between the base pairs facilitate base–base aggregation, thereby controlling the assembly process.

2. Methodology

The MD simulations were performed at the constant-energy, constant-volume (NVT) and isothermal-isobaric (NPT) ensembles in the gas (vacuum) and aqueous phases using the Nanoscale MD package [32]. The all atom Chemistry at Harvard Macromolecular Mechanics (CHARMM27) force field [33] for graphene was employed which include both bonded and nonbonded parameters [34]. The Particle Mesh Ewald [35] summation was used to calculate the periodic electrostatic interactions with a long-range cutoff of 12.0 Å. For aqueous phase, the water molecules were represented by the TIP3P water model with constraints applied to the bond lengths and angles using the SETTLE algorithm. Room temperature (i.e. 298.15 K) simulations were performed using the Langevin dynamics, and the Langevin piston Nose-Hoover method was employed to maintain the pressure to 101.3 kPa.

The free-standing cytosine bases were simulated in a periodic supercell of $(50 \times 50 \times 50)$ Å^3. Calculations incorporated 2000 steps of energy minimization using the conjugate gradient algorithm followed by 50 ns of production run using the NVT and NPT ensembles in gas and aqueous phases. The graphene monolayer was modeled in a periodic supercell of (61.6×62.4) Å^2 comprising of 1500 carbon atoms. The MD simulation of the C_n/graphene incorporated 2000 steps of energy minimization followed by 50 ns of production run at a time step of 1.0 fs. In aqueous phase, we performed simulated annealing with a gradual increment of temperature from 298.15 to 700 K at an interval of 50 K and quenching the system to 298.15 K with a decrement interval of 50 K.

The convergence of the simulation was analyzed using the root mean-square deviation (RMSD) over the trajectory. The RMSD helps in inferring the overall stability of system and a uniform RMSD suggests no major fluctuations in the system. The number of H-bonds provides a qualitative estimate of the average number of H-bonds stabilizing the system. For the last 2 ns of the trajectory, the radial distribution function (RDF) was calculated. The RDF or pair-wise correlation function denoted by $g(r)$ represents the correlation between atom pairs or the probability to find an atom at the distance r of another reference atom. At short distances (less than atomic diameter), the value of $g(r)$ is zero which corresponds to strong repulsive forces. The first large peak demonstrates the likeliness of the two nucleobases to be found at this separation and at long distances, $g(r)$ approaches the value of one which indicates there is no long-range order. The

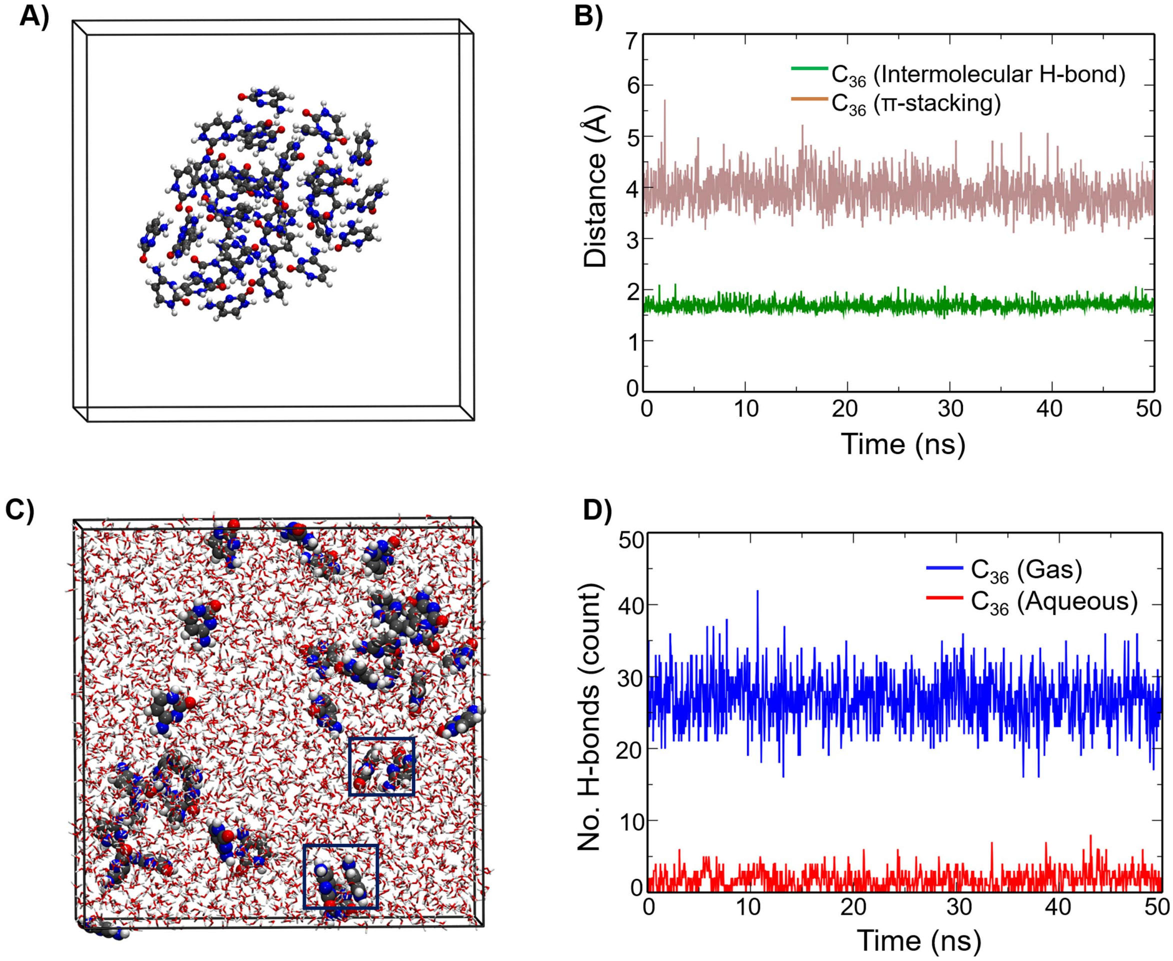

Figure 2. (A) The gas phase snapshot of C_{36} at 50 ns, (B) intermolecular H-bond and π-stacking distances in the gas phase, (C) the aqueous phase snapshot of C_{36} at 50 ns with the π-stacked domains highlighted in the blue squares, and (D) number of H-bonds in the gas and aqueous phases.

normalized RMSD, RDF and the number of H-bonds were calculated with the help of the visual MD [36] plugin.

3. Results and discussion

3.1. Self-assembly of C_n bases

The representative snapshots of free-standing C_n bases (for $n = 2$, 4 and 36) are displayed in figure S1, in the supporting information, which is available online at stacks.iop.org/NANO/29/195601/mmedia, and figure 2(A). In the gas phase, C_2 and C_4 are stabilized by the intermolecular H-bonds (supporting information, figures S1(A) and (B)) while C_{36} prefers to aggregate in a condensed network, stabilized by intermolecular H-bonds and π-stacking interactions. The intermolecular H-bond (base–base) and vdW π-stacking (base–surface) are calculated at $\sim$1.75 and $\sim$4.0 Å as shown in figure 2(B).

In the aqueous phase, the presence of water disrupts the base–base intermolecular interactions resulting in the bases being dispersed. The bases prefer to form π-stacked domains, as highlighted by the blue squares in figure 2(C). Snapshots of C_2 and C_4 in the aqueous phase demonstrate dispersion of the bases with the loss of the intermolecular interactions in presence of water molecules as illustrated in figures S1(C) and (D) of supporting information. This was also predicted in our previous study on the self-assembly of free-standing guanine bases in solvent phase, wherein guanine formed π-stacked domains [37].

To further analyze the predicted stability of free-standing C_n bases, we compared the number of H-bonds in the gas and aqueous phases. The C_2 is stabilized by two H-bonds and C_4 by $\sim$5–6 H-bonds in the gas phase (figure S2(A), supporting information). C_{36} is stabilized by $\sim$28–30 H-bonds in the gas phase as shown in figure 2(D). In the aqueous phase, disruption of the intermolecular interactions between the bases is reflected from a decrease in the number of H-bonds; C_4 with $\sim$1 H-bond (see figure S2(B) of supporting information). For C_{36}, the number of H-bonds drops to $\sim$5, which indicates that the base–base aggregation is driven by the formation of π-stacked domains between the bases.

The overall fluctuations in the RMSD for C_2 and C_4 in the gas phase are calculated to be less than $\sim$1 Å as shown in figures S3(A) and (B) of supporting information. The two break points for C_4 correspond to the configurational reconstruction during the simulation that levels at $\sim$1 Å. For C_{36}, the gas phase RMSD suggests no major fluctuations except

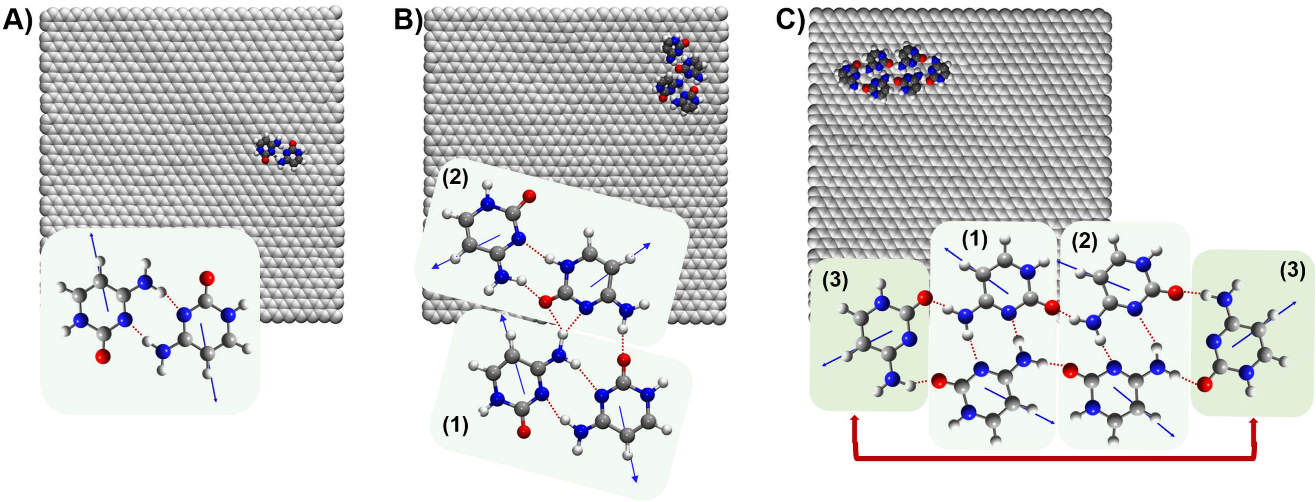

Figure 3. The gas phase snapshots of C_n/graphene at 50 ns; (A) C_2/graphene, (B) C_4/graphene and (C) C_6/graphene. The inset figure demonstrates the alignment of the dipole moment vectors.

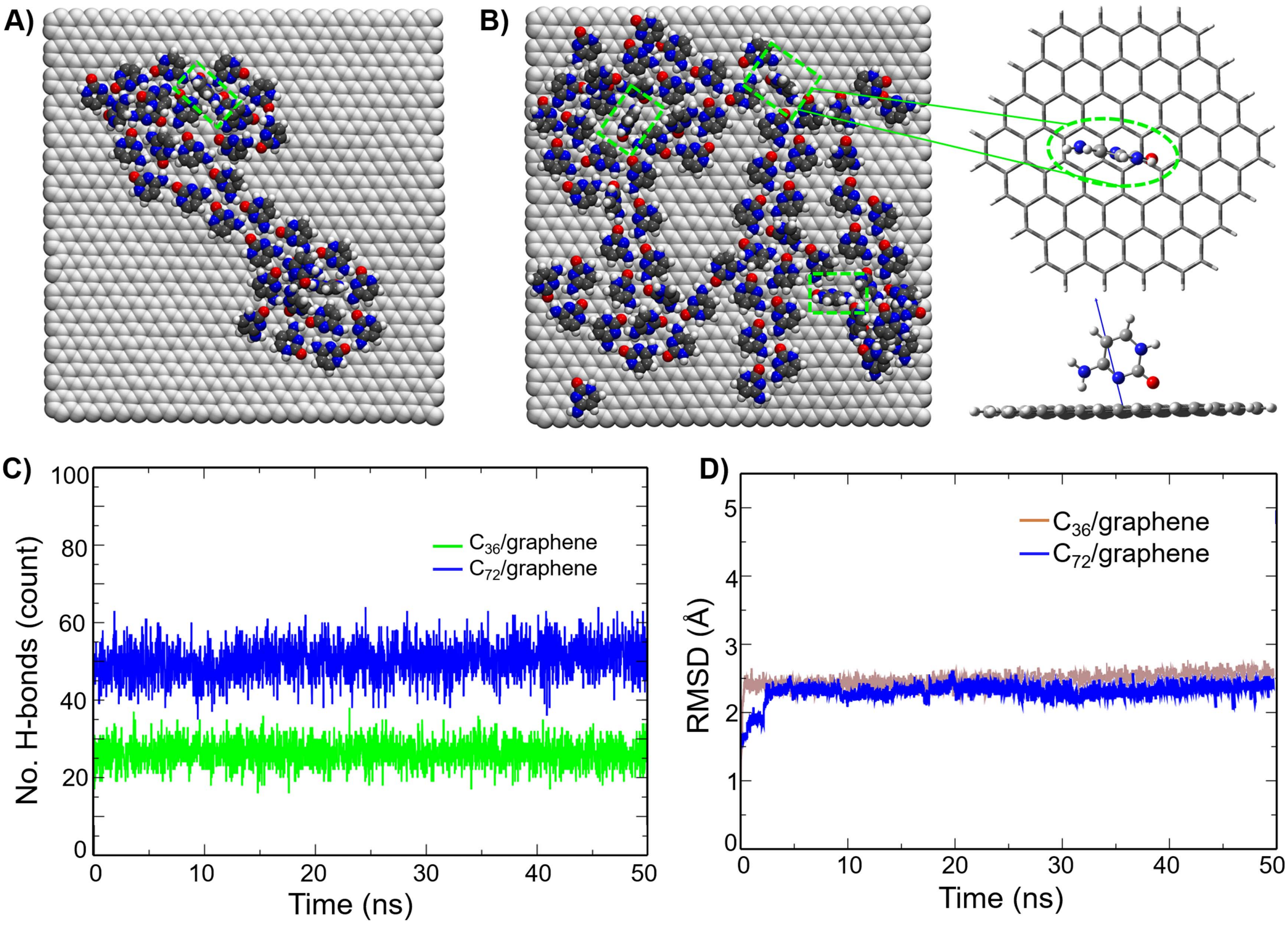

Figure 4. The gas phase snapshot at 50 ns for (A) C_{36}/graphene, and (B) C_{72}/graphene with a depiction of the cytosine/graphene in the perpendicular orientation of interaction. (C) Number of H-bonds, and (D) RMSD for C_{36}/graphene and C_{72}/graphene in the gas phase.

for the first 5 ns of the simulation, and correlates to the structural evolution from a dispersed to a compact (aggregated) network (see figure S3(C) of supporting information). In the aqueous phase, the fluctuations in RMSD is uniform at ~1.0 Å and suggests the overall structural stability of C_{36}.

3.2. Self-assembly of C_n on graphene surface

A periodic graphene monolayer comprising of 1500 atoms was considered to model the self-assembly of C_n bases in the gas and aqueous phases [32]. In the gas phase, for

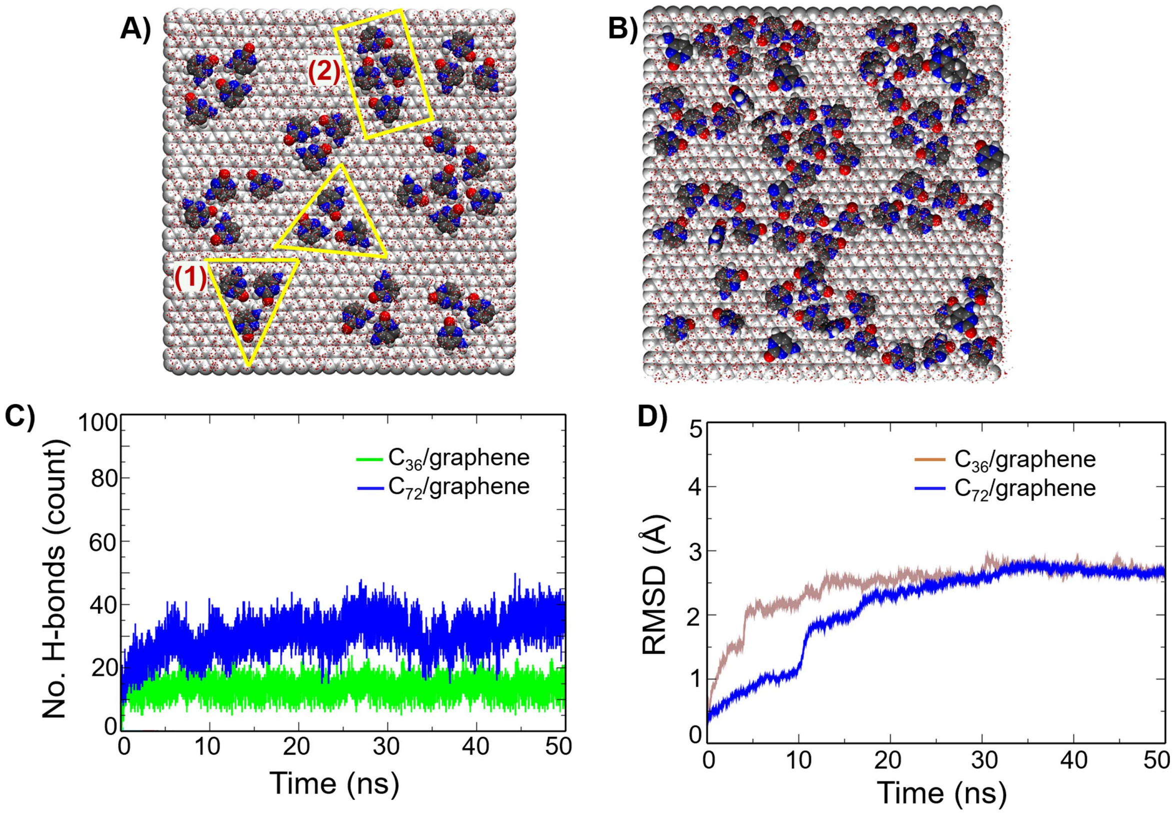

Figure 5. The aqueous phase snapshot at 50 ns for (A) C_{36}/graphene, (B) C_{72}/graphene. (C) Number of H-bonds, and (D) RMSD for C_{36}/graphene and C_{72}/graphene in the aqueous phase.

C_2/graphene (figure 3(A)), the nucleobases tend to dimerize, stabilized by two intermolecular H-bonds as illustrated in the inset figure 3(A). The dipole moment vectors are aligned in an anti-parallel direction. The average π-stacking distance between graphene and cytosine is 3.34 Å, well within the physisorption regime. In C_4/graphene (figure 3(B)), the base pairs are stabilized by the intermolecular H-bonds at an average distance of 1.88 Å. Based on the orientation of cytosine, we find two distinct domains in the assembly, denoted as domains (1) and (2) (see inset figure 3(B)) with the dipole moment vectors aligned anti-parallel to one another. For C_6/graphene (figure 3(C)), the base aggregation can be characterized in three primary domains; in domains (1) and (2), the bases are aligned anti-parallel to each other similar to C_2 while the other two apical bases represented by domain (3) interact simultaneously through the O_{12} and the amine (N_7)-H atoms.

At intermediate surface coverage corresponding to C_{36}/graphene, the bases align in linear arrays, but due to steric hindrances between the bases, some of the bases adopt a perpendicular and titled configuration on graphene as depicted in figure 4(A), green square. The in-plane dipole moment also causes a tilt in orientation of cytosine. For high surface coverage, represented by C_{72}/graphene, most of the bases align in linear arrays in a parallel orientation, while some of the bases adopt both titled and perpendicular orientations as shown in figure 4(B). For the tilted/perpendicular orientation of adsorption, the stabilization is rendered from the intermolecular H-bonds between the bases, rather than the base–surface interaction.

The number of H-bonds in C_n/graphene (figure 4(C)) is similar to the free-standing C_n bases, suggesting that the bases retain the overall H-bond interactions in presence of graphene. This exemplifies that, graphene promotes the monolayer assembly without compromising the intermolecular interactions that govern the overall stabilization between the cytosine bases. The RMSD for C_{36}/graphene and C_{72}/graphene are observed to be uniform at ~2.35–2.50 Å, illustrated in figure 4(D). This demonstrates the stability of the system and that the initial fluctuations in RMSD below 3.0 ns is correlated to the reorientation and relaxation of the bases on graphene.

Our recent study on G_n/graphene[37] predicted that at low surface coverage (i.e. G_6 and G_{12}) the bases are aligned in a linear array with the formation of G_4-quartet motifs. At intermediate coverage (i.e. G_{36}), the bases aggregate in a condensed 2D network in the gas phase. The polarity of guanine coupled with the interaction via alternating donor/acceptor sites facilitates multiple structural arrangements, including the formation of G_4-quartets on graphene. Unlike guanine, which prefers a condensed network with the π-stacking maximized on graphene, cytosine prefers short to medium-range ordered linear arrays. The steric interaction between the bases lead to titling of some of the bases with the dipole moment vector aligned normal to the graphene plane. The predicted trends on free-standing and graphene supported

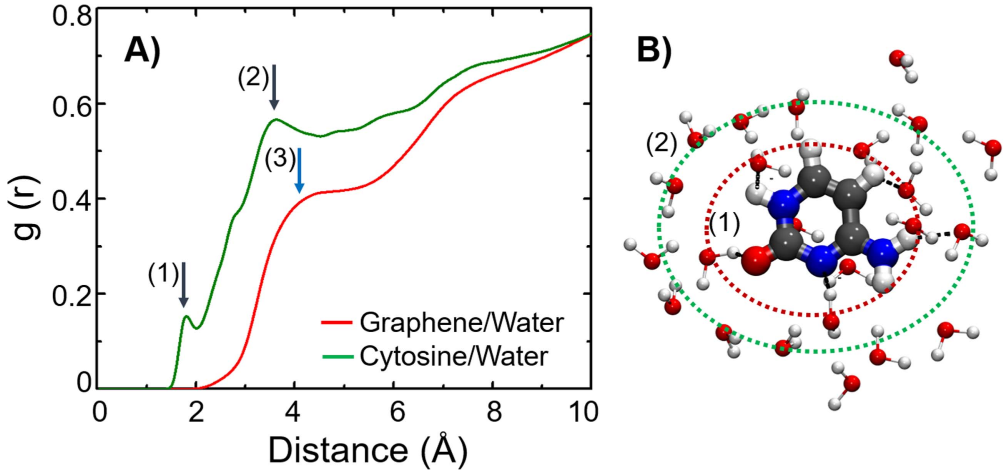

Figure 6. (A) RDF profile between Graphene/Water and Cytosine/Water in the aqueous phase, (B) depiction of the first (1) and second (2) water hydration sphere along cytosine.

C_n/G_n bases suggest that the electronic properties of the DNA bases drive the nature of self-assembly and molecular aggregation on graphene.

In the aqueous phase, at low surface coverage (i.e. C_2/graphene, C_4/graphene and C_6/graphene) the bases are dispersed on graphene with no preferentiality towards base–base aggregation as shown in figure S4 of supporting information. At intermediate surface coverage, corresponding to C_{36}/graphene, the bases aggregate in groups of 3 or 4 as shown in figure 5(A), highlighted in yellow. At high surface coverage, corresponding to C_{72}/graphene (figure 5(B)), the bases aggregate with no well-defined arrays and some of the bases form small groups similar to those observed at intermediate coverage. The polarity of the water solvent media drives the nature of self-assembly of cytosine bases on graphene, and the dipole moment of water disrupts the home-base aggregation by forming hydration spheres around the bases in aqueous phase.

A detailed analysis of the number of H-bonds in the aqueous phase reveals that, in contrast to the free-standing bases, graphene facilitates the base–base interaction. This becomes apparent at intermediate and high surface coverages with an average number of H-bonds of ∼12 and ∼30, respectively as illustrated in figure 5(C). The RMSD as shown in figure 5(D) increases steadily towards the initial phase of the simulation and saturates at ∼2.5 Å beyond 30 ns, with lower fluctuations in the RMSD for C_{36}/graphene. The RMSD plots for C_2/graphene, C_4/graphene and C_6/graphene are provided in the supporting information, figure S5. Substantial fluctuations in RMSD for C_2/graphene in the gas and aqueous phases exhibit the loosely bound bases on graphene. With the increase in the base count, fluctuations in RMSD is uniform below 1.5 Å (see figures S5(B) and (C) of supporting information) with the bases being stabilized on graphene surface.

The RDF is found to be substantial in computing the nearest neighbor distance and the formation of water hydration spheres around C_n and graphene. Figure 6(A) illustrates the RDF profile of C_{36}/graphene, which depicts two characteristic peaks at ∼1.75 Å (label 1) and 3.80 Å (label 2) associated with the two water hydration spheres around cytosine (see figure 6(A)). The RDF for graphene (label 3) shows a single characteristic broad peak around 4.0 Å which corresponds to the water ordering distance on graphene. Around 6 and 12 water molecules constitute the first and second hydration sphere around a representative cytosine as depicted in figure 6(B). This is significantly different from the results obtained for G_n/graphene [37], wherein the guanine nucleobase due to the presence of more H-bond donor and acceptor sites, encompasses around 10 and 18 water molecules in the first and second hydration spheres.

The trends obtained from our MD simulation agree with the first-principles DFT results [38] suggesting that the tilt of the bases is due to the dominance of intermolecular interactions, especially at high surface coverage. Using vdW dispersion-corrected DFT at the wB97XD/6-31 G (d, p) level of theory (see section SI of supporting information), we compared the energy landscape of a cytosine molecule adsorbed on graphene in the perpendicular, tilted and parallel orientations. An agreement was observed with the reported trends, with the parallel configuration being energetically favored compared to the perpendicular and titled configurations, although the energy barrier was shallow for the three configurations (see supporting information, section SII).

The MD simulations in gas phase (figure 3) find the preferred stacking mode to be the parallel orientation of cytosine which enables maximum electron overlap. To affirm this prediction, we now perform DFT calculations for C_2/graphene system as a prototype to investigate the energetics of interaction in this complex. Following the cluster model used to investigate G_2/graphene system, we employ a finite 120 atom model for graphene to investigate its interaction with C_2 dimer [29].

The calculated DFT ground state configuration of C_2/graphene in gas phase is shown in figure 7(A). The C_2 bases are perfectly aligned on graphene at an average interplanar distance of 3.24 Å and has an interaction energy of −1.24 eV. The interaction energy is defined as the difference in

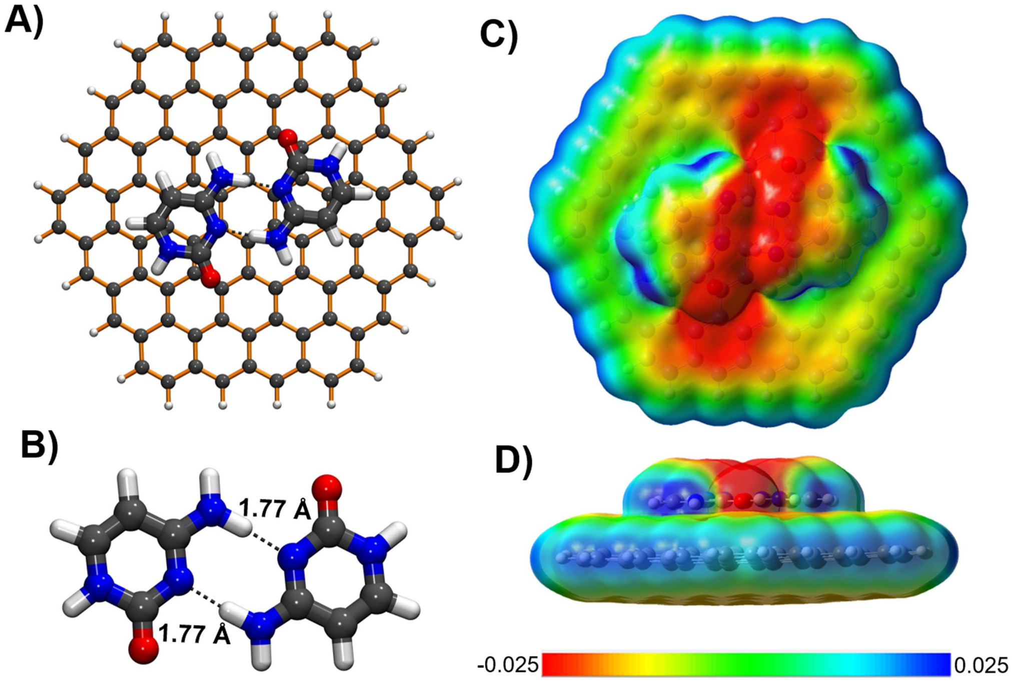

Figure 7. (A) Calculated equilibrium configuration of C_2/graphene, (B) intermolecular H-bond distance between a C_2 dimer in C_2/graphene, and (C and D) side and top views of the ESP isosurface of C_2/graphene in gas phase.

total energy of C_2/graphene complex and total energies of free-standing cytosine dimer and graphene, respectively. Likewise, the inclusion of basis set superposition error correction yields the interaction energy of −0.90 eV in gas phase. The average intermolecular H-bond distance between the C_2 dimer physisorbed on graphene is calculated to be 1.77 Å (see figure 7(B)). Thus, the DFT and MD results are in excellent agreement with each other in predicting the interaction energy for C_2/graphene. Note that the interaction energy value of −1.72 eV was calculated for $(Gua)_2$/graphene system in gas phase at the PBE-D2 level of theory [29].

The ESP isosurface of C_2/graphene (figures 7(C) and (D)) display regions of negative electron density on the O_{12}, N_{10} and N_7 atoms of cytosine, which contribute to the intermolecular H-bond stabilization between the C_2 dimer. Although the regions of intermediate electron density are delocalized on graphene, physisorption of C_2 dimer leads to localized negative charge density on the carbon atoms of graphene in close proximity to the cytosine bases.

We further compare our MD results with prior studies on the self-assembly of cytosine nucleobases on Au (111) and HOPG surfaces. Kelly *et al* [31], reported the assembly of cytosine bases on the Au (111) surface using ultrahigh vacuum STM and *ab initio* DFT. Disordered assemblies of cytosine was observed which connected into bent chains, T-junctions and nanocages. Low and medium surface coverage resulted in zigzag lines and rings on the Au (111). Wandlowski *et al* [39], observed cytosine forming both ordered and disordered phases in solution on the Au (111) surface. Otero *et al* [40], investigated the structures of disordered cytosine network on the Au (111) surface using STM. The cytosine bases lacked a long-range ordered network and formed small number of supramolecular structural motifs with medium-range order. Besenbacher *et al* reported the adsorption and co-adsorption of guanine and cytosine bases at the 1-octanol/graphite interface using *in situ* STM [41]. The cytosine bases were aligned in parallel and straight rows. They were stabilized by the intermolecular H-bonds with a tilt angle of 60° between the two linear domains.

The calculated results provide atomistic insights towards the molecular ordering and self-assembly of C_n bases on graphene. The bases have preference for ordered, short-range linear arrays. Except for the aqueous phase results that demonstrate complete immobilization and disruption of the base–base interaction at low surface coverage and disordered orientations at intermediate and high surface coverage, the predicted trends from the gas phase simulation elucidate the role and dominance of graphene in mediating the monolayer self-assembly of cytosine into linear arrays with medium-range order. The self-assembly is found to correlate with the nature of the surface, especially in the way the bases prefer to align and assemble. In the gas phase, we observed the bases to orient anti-parallel while Otero *et al*, predicted three elementary structural motifs of C_n on the Au(111) surface; zigzag filaments, five-fold and six-fold rings [40]. The intermolecular H-bonding primarily stabilizes the self-assembly of C_n on graphene with short-to-medium range molecular ordering.

It is well known that the H-bond strength of DNA bases which is controlled by the ionization constant (pK_a) determines the extent of base-pairing and whether the imine nitrogen atoms can function as H-donors or acceptors [42]. In general, pK_a values suggest that the DNA bases remain in neutral (canonical) form under the physiological conditions within the range of $5 < pH < 9$ [43, 44]. Cytosine, thymine and uracil are the naturally occurring pyrimidines that exist in the keto (lactam) form at neutral pH. The keto form of cytosine is stable at physiological pH, while in acidic pH, the N_{10} atom is protonated with $pK_{a1} = 4.45$ [45], giving cytosine a positive charge impeding base pairing. The change in protonation state tends to decreases the stability of cytosine [46–49].

4. Summary

In summary, the present study provides qualitative and fundamental insights on the dominant interactions that determine the self-assembly of cytosine nucleobases on graphene. A detailed understanding on the self-assembly of canonical versus noncanonical DNA bases could be substantial towards unraveling the mechanisms that control the medium to long-range ordering on 2D nanomaterials and serve as fingerprints to differentiate between noncanonical DNA base pair combinations. The study exemplifies an important approach towards understanding the molecular recognition, aggregation dynamics and growth of noncanonical DNA nucleobases on graphene and similar 2D functional nanomaterials.

The future direction of the research is the integration of self-assembled nanostructures for biosensing applications. The ability to regulate the assembly into well-defined patterns would constitute the first step towards assimilating self-organized hierarchical nanostructures in the next-generation DNA based biosensors and nanoelectronic devices [50–52]. The graphene field effect transistors are one of the examples of nanoelectronic devices [53, 54] which were successfully fabricated for the ultrasensitive, label-free detection of DNA nucleobases [55–60].

Acknowledgments

The authors are grateful to Prof Max Seel and Dr S Gowtham of Michigan Technological University for the helpful discussions. NS acknowledges financial support from Michigan Technological University. The Superior high-performance computing cluster at Michigan Technological University was utilized in obtaining the results presented in the study.

Notes

The authors declare no competing financial interest.

ORCID iDs

Nabanita Saikia https://orcid.org/0000-0002-0684-260X
Kevin Waters https://orcid.org/0000-0003-3828-8647
Ravindra Pandey https://orcid.org/0000-0002-2126-1985

References

[1] Hamley I W and Castelletto V 2017 Self-assembly of peptide bioconjugates: selected recent research highlights *Bioconjugate Chem.* **28** 731–9
[2] Gottarelli G, Masiero S, Mezzina E, Pieraccini S, Rabe J P, Samori P and Spada G P 2006 The self-assembly of lipophilic guanosine derivatives in solution and on solid surfaces *Chem. Eur. J.* **6** 3242–8
[3] Jasinski D, Haque F, Binzel D W and Guo P 2017 Advancement of the emerging field of RNA nanotechnology *ACS Nano* **11** 1142–64
[4] Rodes A, Rueda M, Prieto F, Prado C, Feliu J M and Aldaz A 2009 Adenine adsorption at single crystal and thin-film gold electrodes: an *in situ* infrared spectroscopic study *J. Phys. Chem.* C **113** 18784–94
[5] Zhu C, Yang G, Li H, Du D and Lin Y 2015 Electrochemical sensors and biosensors based on nanomaterials and nanostructures *Anal. Chem.* **87** 230–49
[6] Friend R H *et al* 1999 Electroluminescence in conjugated polymers *Nature* **397** 121–8
[7] Carneiro C E A *et al* 2011 Adsorption of adenine, cytosine, thymine, and uracil on sulfide-modified montmorillonite: FT-IR, Mössbauer and EPR spectroscopy and x-ray diffractometry studies *Orig. Life Evol. Biosph.* **41** 453–68
[8] Akdim B, Pachter R, Day P N, Kim S S and Naik R R 2012 On modeling biomolecular-surface nonbonded interactions: application to nucleobase adsorption on single-wall carbon nanotube surfaces *Nanotechnology* **23** 165703
[9] Otero R, Schöck M, Molina L M, Laegsgaard E, Stensgaard I, Hammer B and Besenbacher F 2005 Guanine quartet networks stabilized by cooperative hydrogen bonds *Angew. Chem., Int. Ed. Engl.* **44** 2270–5
[10] Kilina S, Tretiak S, Yarotski D A, Zhu J-X, Modine N, Taylor A and Balatsky A V 2007 Electronic properties of DNA base nucleobases adsorbed on a metallic surface *J. Phys. Chem.* C **111** 14541–51
[11] Maleki A, Alavi S and Najafi B 2011 Molecular dynamics simulation study of adsorption and patterning of DNA bases on the Au(111) surface *J. Phys. Chem.* C **115** 22484–94
[12] Kelly R E A, Xu W, Lukas M, Otero R, Mura M, Lee J Y, Lægsgaard E, Stensgaard I, Kantorovich L N and Besenbacher F 2008 An investigation into the interactions between self-assembled adenine nucleobases and a Au(111) surface *Small* **4** 1494–500
[13] Barone V, Casarin M, Forrer D, Monti S and Prampolini G 2011 Molecular dynamics simulations of the self-assembly of tetraphenylporphyrin-based monolayers and bilayers at a silver interface *Phys. Chem.* C **115** 18434–44
[14] Chen Q, Frankel D J and Richardson N V 2002 Self-assembly of adenine on Cu(110) surfaces *Langmuir* **18** 3219–25
[15] Tanaka H, Nakagawa T and Kawai T 1996 Two-dimensional self-assembly of DNA base nucleobases on Cu (111) surfaces *Surf. Sci.* **364** L575–9
[16] Freund J E, Edelwirth M, Kröbel P and Heckl W M 1997 Structure determination of two-dimensional adenine crystals on graphite *Phys. Rev.* B **55** 5394
[17] Kumar A M S, Fox J D, Buerkle L E, Marchant R E and Rowan S J 2009 Effect of monomer structure and solvent on the growth of supramolecular nanoassemblies on a graphite surface *Langmuir* **25** 653–6
[18] Heckl W M, Smith D P E, Binnig G, Klagges H, Hansch T W and Maddocks J 1991 Two-dimensional ordering of the DNA base guanine observed by scanning tunneling microscopy *Proc. Natl Acad. Sci.* **88** 8003–5
[19] Lin Q, Zou X, Zhou G, Liu R, Wu J, Li J and Duan W 2011 Adsorption of DNA/RNA nucleobases on hexagonal boron nitride sheet: an *ab initio* study *Phys. Chem. Chem. Phys.* **13** 12225–30
[20] Ding N, Chen X, Wu C-M L and Li H 2013 Adsorption of nucleobase pairs on hexagonal boron nitride sheet: hydrogen bonding versus stacking *Phys. Chem. Chem. Phys.* **15** 10767–76

[21] van Mourik T, Bühl M and Gaigeot M-P 2014 Density functional theory across chemistry, physics and biology *Philos. Trans.* A **372** 20120488
[22] Zhao Y, Wu Q, Chen Q and Wang J 2015 Molecular self-assembly on two-dimensional atomic crystals: insights from molecular dynamics simulation *J. Phys. Chem. Lett.* **6** 4518–24
[23] Akca S, Foroughi A, Frochtzwajg D and Postma H W C 2011 Competing interactions in DNA assembly on graphene *PLoS One* **6** e18442
[24] De Feyter S and Schryver De Frans C 2003 Two-dimensional supramolecular self-assembly probed by scanning tunneling microscopy *Chem. Soc. Rev.* **32** 139–50
[25] Kumar A, Banerjee K and Liljeroth P 2017 Molecular assembly on two-dimensional materials *Nanotechnology* **28** 082001
[26] Reuven D G, Shashikala H B M, Mandal S, Williams M N V, Chaudhary J and Wang X-Q 2013 Supramolecular assembly of DNA on graphene nanoribbons *J. Mater. Chem.* B **1** 3926–31
[27] Reddy G N M, Marsh A, Davis J T, Masiero S and Brown S P 2015 Interplay of noncovalent interactions in ribbon-like guanosine self-assembly: an NMR crystallographic study *Cryst. Growth Des.* **15** 5945–54
[28] Zhang Z, Huang H, Yang X and Zang L 2011 Tailoring electronic properties of graphene by π–π stacking with aromatic nucleobases *J. Phys. Chem. Lett.* **2** 2897–905
[29] Saikia N, Karna S P and Pandey R 2017 Theoretical study of gas and solvent phase stability and molecular adsorption of noncanonical guanine bases on graphene *Phys. Chem. Chem. Phys.* **19** 16819–30
[30] Hunter K C, Rutledge L R and Wetmore S D 2005 The hydrogen bonding properties of cytosine: a computational study of cytosine complexed with hydrogen fluoride, water, and ammonia *J. Phys. Chem.* A **109** 9554–62
[31] Kelly R E A, Lukas M, Kantorovich L N, Otero R, Xu W, Mura M, Lægsgaard E, Stensgaard I and Besenbacher F 2008 Understanding the disorder of the DNA base cytosine on the Au(111) surface *J. Chem. Phys.* **129** 184707
[32] Phillips J C, Braun R, Wang W, Gumbart J, Tajkhorshid V E, Chipot C, Skeel R D, Kale L and Schulten K 2005 Scalable molecular dynamics with NAMD *J. Comput. Chem.* **26** 1781–802
[33] Kang Y, Wang Q, Liu Y-C, Shen J-W and Wu T 2010 Diameter selectivity of protein encapsulation in carbon nanotubes *J. Phys. Chem.* B **114** 2869–75
[34] Deshmukh S A, Kamath G and Sankaranarayanan S K R S 2014 Comparison of the interfacial dynamics of water sandwiched between static and free-standing fully flexible graphene sheets *Soft Matter* **10** 4067–83
[35] Darden T, York D and Pedersen L 1993 Particle-mesh Ewald: an N.log(N) method for Ewald sums in large systems *J. Chem. Phys.* **98** 10089–92
[36] MacKerell A D Jr *et al* 1998 All-atom empirical potential for molecular modeling and dynamics studies of proteins *J. Phys. Chem* B **102** 3586–616
[37] Saikia N, Waters K, Karna S P and Pandey R 2017 Hierarchical self-assembly of noncanonical guanine nucleobases on graphene *ACS Omega* **2** 3457–66
[38] Yin Y, Cervenka J and Medhekar N V 2017 Molecular dipole-driven electronic structure modifications of DNA/RNA nucleobases on graphene *J. Phys. Chem. Lett.* **8** 3087–94
[39] Wandlowski T, Lampner D and Lindsay S M 1996 Structure and stability of cytosine adlayers on Au(111): an *in situ* STM study *J. Electroanal. Chem.* **404** 215
[40] Otero R, Lukas M, Kelly R E A, Xu W, Lægsgaard E, Stensgaard I, Kantorovich L N and Besenbacher F 2008 Elementary structural motifs in a random network of cytosine adsorbed on a gold(111) surface *Science* **319** 312
[41] Xu S, Dong M, Rauls E, Otero R, Linderoth T R and Besenbacher F 2006 Coadsorption of guanine and cytosine on graphite: ordered structure based on GC pairing *Nano Lett.* **6** 1434–8
[42] Sanger W 1984 *Principles of Nucleic Acid Structure* (New York: Springer) pp 105–40
[43] Ganguly S and Kundu K K 1994 Protonation/deprotonation energetics of uracil, thymine, and cytosine in water from e.m.f./spectrophotometric measurements *Can. J. Chem.* **72** 1120–6
[44] Singh V, Fedeles B I and Essigmann J M 2015 Role of tautomerism in RNA biochemistry *RNA* **21** 1–13
[45] Shugar D and Fox J J 1952 Spectrophotometric studies op nucleic acid derivatives and related compounds as a function of pH *Biochim. Biophys. Acta* **9** 199–218
[46] Vieregg J R 2010 Nucleic acid structural energetics *Encyclopedia of Analytical Chemistry* ed R A Meyers (New York: Wiley) pp 1–17
[47] Lang J, Strum J and Zana R 1973 Ultrasonic absorption in aqueous solutions of nucleotides and nucleosides: I. Effect of pH and concentration *J. Phys. Chem.* **77** 2329–34
[48] Sturm J, Lang J and Zana R 1971 Ultrasonic absorption of DNA solutions: influence of pH *Biopolym.* **10** 2639–43
[49] Krishnamurthy R 2012 Role of pK_a of nucleobases in the origins of chemical evolution *Acc. Chem. Res.* **45** 2035–44
[50] Ping J, Vishnubhotla R, Vrudhula A and Charlie Johnson A T 2016 Scalable production of high-sensitivity, label-free DNA biosensors based on back-gated graphene field effect transistors *ACS Nano* **10** 8700–4
[51] Norton M 2007 Designed self-organization for molecular optoelectronic sensors *Int. J. High Speed Electron. Syst.* **17** 311–26
[52] Gothelf K V and LaBean T H 2005 DNA-programmed assembly of nanostructures *Org. Biomol. Chem.* **3** 4023–37
[53] Tapio K, Leppiniemi J, Shen B, Hytönen V P, Fritzsche W and Toppari J J 2016 Toward single electron nanoelectronics using self-assembled DNA structure *Nano Lett.* **16** 6780–6
[54] Dong X, Shi Y, Huang W, Chen P and Li L J 2010 Electrical detection of DNA hybridization with single-base specificity using transistors based on CVD-grown graphene sheets *Adv. Mater.* **22** 1649–53
[55] Bellido E P, Bobadilla A D, Rangel N L, Zhong H, Norton M L and Seminario A S J M 2009 Current–voltage–temperature characteristics of DNA origami *Nanotechnology* **20** 175102
[56] Zheng C, Huang L, Zhang H, Sun Z, Zhang Z and Zhang G-J 2015 Fabrication of ultrasensitive field-effect transistor DNA biosensors by a directional transfer technique based on CVD-grown graphene *ACS Appl. Mater. Interfaces* **7** 16953–9
[57] Jin Z, Sun W, Ke Y, Shih C-J, Paulus G L C, Wang Q H, Mu B, Yin P and Strano M S 2013 Metallized DNA nanolithography for encoding and transferring spatial information for graphene patterning *Nat. Commun.* **4** 1663
[58] Heerema S J and Dekker C 2016 Graphene nanodevices for DNA sequencing *Nat. Nanotechnol.* **11** 127–36
[59] Ahmed T, Kilina S, Das T, Haraldsen J T, Rehr J J and Balatsky A V 2012 Electronic fingerprints of DNA bases on graphene *Nano Lett.* **12** 927–31
[60] Bobadilla A D and Seminario J M 2011 DNA-CNT interactions and gating mechanism using MD and DFT *J. Phys. Chem.* C **115** 3466–74